PROF. LILI HUANG (Orcid ID : 0000-0002-7085-7646)

Article type : Regular Manuscript

A receptor-like protein from *Nicotiana benthamiana* mediates VmE02 PAMP-triggered immunity

Authors

Jiajun Nie[1], Wenjing Zhou[1], Jianying Liu[1], Ni Tan[1], Jian-Min Zhou[2], Lili Huang[1,*]

Affiliation

[1]State Key Laboratory of Crop Stress Biology for Arid Areas, College of Plant Protection, Northwest A&F University, Yangling, Shaanxi 712100, China

[2]State Key Laboratory of Plant Genomics, Institute of Genetics and Developmental Biology, Chinese Academy of Sciences, Beijing 100101, China

[*]**Correspondence:**

Lili Huang, Tel: +86 29 8709 1312; e-mail: huanglili@nwsuaf.edu.cn

Received: *21 April 2020*

Accepted: *4 October 2020*

ORCID ID: 0000-0002-7085-7646 (L.H.)

ORCID ID: 0000-0002-5765-0931 (J.N.)

ORCID ID: 0000-0002-9943-2975 (J.-M.Z.)

Summary

Plants employ innate immune system to defend against phytopathogens. As a part, pattern triggered-immunity is activated via pattern recognition receptors (PRRs) detection of pathogen-associated molecular patterns (PAMPs). While with an increasing number of PAMPs being identified, the PRRs for their recognition remain largely unknown.

In the present study, we report a receptor-like protein RE02 (Response to VmE02) in *Nicotiana benthamiana*, which mediates the perception of VmE02, a PAMP previously identified from the phytopathogenic fungus *Valsa mali*, using virus-induced gene silencing (VIGS), co-immunoprecipitation, pull-down and microscale thermophoresis assays.

We showed that, silencing of *RE02* markedly attenuated VmE02-triggred cell death and immune responses. RE02 specifically interacted with VmE02 *in vivo* and *in vitro*, and it displayed a high affinity for VmE02. Formation of a complex with the receptor-like kinases SOBIR1 and BAK1 was essential for RE02 to perceive VmE02. Moreover, *RE02*-silenced plants exhibited enhanced susceptibility to both the oomycete *Phytophthora capsici* and the fungus *Sclerotinia sclerotiorum*, while overexpression of RE02 increased plant resistance to these pathogens.

Taken together, our results indicate that the PAMP VmE02 and the receptor-like protein RE02 represent a new ligand-receptor pair in plant immunity, and RE02 represents a promising target for engineering disease resistance.

Key words: pattern recognition receptor, receptor-like protein, plant innate immunity, virus-induced gene silencing, *Nicotiana benthamiana*.

Introduction

Plants are constantly threatened by large amounts of microbial pathogens. In response to pathogen attacks, plants have evolved a multifaceted immune system during continuous coevolution. As part of this, plants employ pattern recognition receptors (PRRs) at cell surface to

detect pathogen-associated molecular patterns (PAMPs), which are evolutionarily conserved molecules essential for microbial viability or fitness, triggering innate immune responses and limiting pathogen infection (Akira *et al.*, 2006; Boutrot & Zipfel, 2017; Tang *et al.*, 2017; Albert *et al.*, 2020).

Plant PRRs mostly belong to receptor-like kinases (RLKs) or receptor-like proteins (RLPs), both of which often contain leucine-rich repeat (LRR) ectodomains required for extracellular ligand binding (Shiu *et al.*, 2004; Fritz-Laylin *et al.*, 2005; Wang *et al.*, 2008; Couto & Zipfel, 2016). The best-characterized RLK-type PRRs include FLS2 and EFR from *Arabidopsis*, which are responsible for recognition of bacterial flagellin (flg22) and elongation factor Tu (elf18), respectively (Gómez-Gómez & Boller, 2000; Chinchilla *et al.*, 2006; Zipfel *et al.*, 2006; Sun *et al.*, 2013). Other well-known RLK-type PRRs include FLS3 from tomato detecting flgII-28, a flagellin epitope distinct from flg22 (Hind *et al.*, 2016), XPS1 from *Arabidopsis* recognizing the xup25 peptide among a bacterial xanthine/uracil permease (Mott *et al.*, 2016), and XA21 in rice perceiving the tyrosine-sulfated protein RaxX from *Xanthomonas oryzae* pv. *oryzae* (Pruitt *et al.*, 2015), etc. Distinct from RLKs, RLPs lack any obvious kinase domain for intracellular signaling. Whereas, various RLPs function as PRRs to mediate plant innate immunity as well. For example, the typical RLPs Eix2, Ve1 and Cfs from tomato separately mediate recognition of fungal ethylene-inducing xylanase (EIX), *Cladosporium fulvum* AVRs and *Verticillium dahliae* Ave1 (Ron & Avni, 2004; de Jonge *et al.*, 2012; de Wit PJ. 2016); RLP23, RLP30, RLP42, and ReMAX in *Arabidopsis* recognize the nlp20 epitope among necrosis and ethylene-inducing proteins (NLPs), SCFE1 elicitor from *Sclerotinia sclerotiorum*, endopolygalacturonases from *Botrytis cinerea* and *Aspergillus niger*, and eMax from *Xanthomonas*, respectively (Jehle *et al.*, 2013; Zhang *et al.*, 2013; Zhang *et al.*, 2014; Albert *et al.*, 2015); ELR from a wild potato species (*Solanum microdontum*) perceives INF1 elicitin (Du *et al.*, 2015); NbCSPR from *Nicotiana benthamiana* participates in cold-shock protein detection (Saur *et al.*, 2016), though the RLK CORE from Solanaceae plants also mediates its recognition (Wang *et al.*, 2016). Most recently, *N. benthamiana* RXEG1 has been demonstrated to perceive the glycoside hydrolase XEG1 from *Phytophthora sojae* (Wang *et al.*, 2018). Despite these profound findings, a vast majority of the

putative receptors remain largely elusive with regard to their corresponding ligands. On the other hand, an increasing number of microbial PAMPs have been identified, with their surface receptors uncharacterized. It is crucial and urgent to match the ligand-receptor pairs in plant immunity research.

PRR perception of a cognate PAMP usually confers host plants a broad-spectrum resistance against multiple pathogens, which can be exploited in plant disease control using genetics method (Dangl *et al.*, 2013; Boutrot & Zipfel, 2017). For example, interspecies transfer of *Arabidopsis* EFR promotes tomato resistance to *Ralstonia solanacearum* and *Xanthomonas perforans* (Lacombe *et al.*, 2010). Similarly, transgenic expression of RLP23 in tomato confers enhanced resistance to both *Phytophthora infestans* and *S. sclerotiorum* (Albert *et al.*, 2015). Moreover, modular assembly of an EFR-Cf-9 chimeric receptor greatly boosts tobacco resistance to bacterial pathogens (Wu *et al.*, 2019). Hence, characterization of the PRRs of PAMPs would be promising for engineering efficient disease resistance.

Multiple strategies have been employed to identify PRRs in plants, of which, forward and reverse genetics are the most productive ones (Boutrot & Zipfel, 2017). As classic examples of forward genetics, FLS2 was identified from an ethyl methanesulfonate (EMS)-mutagenized population of the flagellin-sensitive *Arabidopsis* ecotype (Gómez-Gómez & Boller, 2000), and FLS3 was identified from natural variations of tomato varieties (Hind *et al.*, 2016). The chitin receptor LYK5 and CERK1 were identified by T-DNA mutants of LysM-containing RLKs and RLPs, being the well-known examples of reverse genetics (Miya *et al.*, 2007; Cao *et al.*, 2014). Importantly, Wang and colleagues recently developed a reverse genetics method by genome-wide silencing of RLKs and RLPs in *N. benthamiana* to identify RXEG1 as XEG1 receptor, which provides an efficient toolkit to match new plant immune receptors (Wang *et al.*, 2018). Apart from genetics, several PRRs were characterized by biochemical methods. For example, using photoaffinity labeling and affinity cross-linking, a chitin-binding protein which was later identified to be the chitin receptor OsCEBiP in rice was characterized (Ito *et al.*, 1997; Kaku *et al.*, 2006). Likewise, PEPR1, a receptor for *Arabidopsis* endogenous peptide elicitor AtPEP1 was isolated (Yamaguchi *et al.*, 2006). Furthermore, using the co-receptor BAK1 as a molecular bait, NbCSPR

was successfully identified (Saur *et al.*, 2016).

Previously, we found that VmE02, a small cysteine-rich protein identified in apple Valsa canker pathogen *Valsa mali*, is recognized as a novel PAMP (Nie *et al.*, 2019). VmE02 is capable of triggering cell death in multiple plant species including its apple host (*Malus domestica*) and the nonhost *N. benthamiana* (Nie *et al.*, 2019). VmE02 homologues are widely spread in both fungi and oomycetes, many of which also exhibits cell death-inducing activity (Nie *et al.*, 2019). Here in this study, we adopted virus-induced gene silencing (VIGS) to knock down typical RLP-encoding genes in *N. benthamiana*, and identified an RLP RE02 (Response to VmE02) that is indispensable for VmE02-triggered cell death. Our results further indicate that RE02 functions as a receptor of VmE02 to mediate VmE02-induced immune responses and positively regulate plant resistance against filamentous phytopathogens such as *Phytophthora capsici* and *S. sclerotiorum*.

Materials and Methods

Bacterial strains and plasmid construction

Escherichia coli strainTop10 and *Agrobacterium tumefaciens* strain GV3101 were used for cloning and plant transformation, respectively. Silencing fragments (Wang *et al.*, 2018) and overexpression sequences were amplified from cDNA library of *N. benthamiana* with gene-specific primers (Table S1), using Phusion High-Fidelity DNA Polymerase (New England Biolabs, Ipswich, MA, USA). VmE02 homologous sequences and INF1 were cloned from previous PVX plasmids (Nie *et al.*, 2019). The purified amplicons were ligated with TRV2, pCAMBIA1302-*GFP*, or pICH86988-*mcherry* vectors digested with specific enzymes, using ClonExpress II One-Step Cloning Kit (Vazyme, Nanjing, China). Both gene-silencing and binary plasmid constructs were mobilized into *A. tumefaciens* GV3101 by electroporation.

Plant growth and agroinfiltration

N. benthamiana plants were grown in a climate chamber (16 h photoperiod, 22°C, 65% relative humidity). *A. tumefaciens* strain GV3101 carrying binary or silencing vectors were cultured on Lysogeny Broth (LB) medium supplemented with appropriate antibiotics at 28°C. The

bacteria cells were pelleted and resuspended in MES buffer (10 mM $MgCl_2$, 10 mM 2-(N-morpholino) ethane sulfonic acid MES, 200 μM acetosyringone, pH 5.7) in the dark for 3 h at room temperature (RT) before infiltration. For transient expression assays, suspended *A. tumefaciens* cells were mixed with P19 silencing suppressor at appropriate ratio to a final OD_{600} of 0.6, followed by infiltration in six-week-old *N. benthamiana* leaves using a syringe without a needle. For TRV (tobacco rattle virus)-mediated gene silencing, *A. tumefaciens* cultures expressing TRV2 constructs and those expressing TRV1 were mixed at 1:1 ratio to a final OD_{600} of 0.8 before injection into primary leaves of four-leaf-stage *N. benthamiana* seedlings. TRV2:*PDS* and TRV:*GFP* were used as controls. Three weeks after TRV2 constructs treatment, plants were used for corresponding assays.

Recombinant protein expression and purification

His-tagged VmE02 was expressed and purified as described (Nie *et al.*, 2019). His-tagged RE02 LRR domains ($RE02^{LRR}$) and RLP23 LRR domains ($RLP23^{LRR}$) were expressed similarly with minor modifications. Briefly, the coding sequence of $RE02^{LRR}$ and $RLP23^{LRR}$ were individually cloned into pET28a vector (Novagen, United States), and the expression constructs were subsequently mobilized in *E. coli* strain BL21(DE3). Protein expressions were induced by adding 0.3 mM isopropyl-β-D-thiogalactopyrandoside (IPTG) in LB medium. After cultivation at 200 rpm, 16°C for 24 h, bacterial cells were collected and washed twice with ultra-pure distilled water by centrifugation at 5,000 g for 10 min. The collected samples were resuspended in PBS buffer (20 mM Na_2HPO_4, 300 mM NaCl, pH 7.4) with 6 M guanidine hydrochloride and 1 mM PMSF, followed by incubation at RT for 1 h. The supernatant containing denatured proteins was then obtained by sonication and centrifugation at 8,000 g for 10 min. Proteins were purified using Ni-NTA resin (Thermo Scientific, Waltham, MA, USA) following the manufacturer's instructions. To refold these proteins, the samples were stepwise dialyzed against PBS buffer with descending concentration of guanidine hydrochloride (from 4 M to 0 M), pH 7.4. After dialysis, the protein samples were concentrated using centrifugal filter devices with appropriate molecular mass (Millipore).

Peptide materials

Flg22 peptide was purchased from Genscript, and csp22 peptide was synthesized by GenScript (Genscript Biotech Corporation, China; https://www.genscript.com.cn/). All peptides were dissolved in ultra-pure distilled water for assays.

Measurement of ROS burst

Reactive oxygen species (ROS) production upon PAMP treatment was measured as described (Sang & Macho, 2017). Leaf discs were collected from 4- to 5-week-old *N. benthamiana* plants and floated overnight in 100 µL of ultra-pure distilled water in a 96-well plate. The following day, water was replaced with 100 µL reaction solution containing 100 µM L-012 (a more sensitive derivative of luminol) (Wako Chemical, Japan), 20 µg mL^{-1}peroxidase (Solarbio, Beijing, China), and 1 µM elicitors (Flg22, csp22, or VmE02 purified protein). Luminescence was measured using a Varioskan LUX multimode microplate reader (Thermo Scientific). Eight biological replicates were used for each sample, and the experiments were repeated independently for more than three times. The data for each sample were represented with both relative luminescence units (RLU) and total accumulation of RLU following the described protocol (Sang & Macho, 2017).

Microscale thermophoresis assay

$RE02^{LRR}$ and $RLP23^{LRR}$ were purified and labelled with the Monolith NT™ Protein Labeling Kit RED (Nanotemper Technologies, Germany; https://nanotempertech.com/) according to the instructions provided by the manufacturer. Labeled proteins were incubated with equal volumes of 16 serial dilutions of purified VmE02, flg22 or csp22 peptide for 30 min at RT. Standard treated capillaries (Nanotemper Technologies) were loaded and the measurements were performed by Monolith NT.115 (Nanotemper Technologies). Each assay was carried out at least three biological repeats and multiple technical repeats, and data were analyzed by MO. Affinity Analysis v2.3.0 software.

RNA isolation and qRT-PCR analysis

Total RNA was isolated from *N. benthamiana* using Quick RNA isolation Kit (Huayueyang, Beijing, China) according to the manufacturer's instructions, and first-strand cDNA was synthesized using the RevertAid First Strand cDNA Synthesis Kit (Thermo Scientific, Waltham, MA, USA). Quantitative reverse transcription-PCR (qRT-PCR) was performed with a LightCycler 96 System (Roche, Germany) using RealStar Green Mixture (GenStar, Beijing, China). *NbActin* was used as an internal control to normalize the gene expression. Relative expression levels were determined using the $2^{-\Delta\Delta CT}$ method (Livak & Schmittgen, 2001).

Pathogen inoculation assays

Phytophthora capsici strain LT263 and *Sclerotinia sclerotiorum* strain 1980, both of which contain close VmE02 homologues (Table S2), were used for inoculation on *N. benthamiana*. Before inoculation, *P. capsici* was maintained on 20% (v/v) V8 juice agar for 48 h, and *S. sclerotiorum* was maintained on potato dextrose agar (PDA) for 72 h, both at 25 °C in the dark. *N. benthamiana* leaves at the same position of each plant were collected and inoculated with fresh mycelial plugs (diameter 0.5 cm). Inoculated leaves were then put in a transparent box to maintain high humidity, and the box was kept in the dark for the first 24 h. The lesion diameters of *S. sclerotiorum* were measured 24 h post-inoculation (hpi). To determine disease progression of *P. capsici*, *N. benthamiana* leaf disks (diameter 4 cm) from infection sites were collected 36 hpi, and genomic DNA was isolated for analysis of relative biomass using qRT-PCR as described (Yu *et al.*, 2012). Each assay was repeated at least three times with three independent biological replicates.

Co-immunoprecipitation and western blotting

Agroinfiltrated *N. benthamiana* leaves were harvested 36 h post agroinfiltration (hpa), frozen in liquid nitrogen and ground to fine powder. Total protein was extracted using lysis buffer (50 mM Tris, 150 mM NaCl, 1 mM ethylenediaminetetraacetic acid (EDTA), 5% glycerol, 5 mM dithiothreitol (DTT), 0.5% TritonX-100, 1 mM phenylmethanesulfonyl fluoride (PMSF) and 1%

proteinase inhibitor cocktail (Sigma-Aldrich, St Louis, MO, USA), pH7.5). After centrifugation at 20,000 *g* for 30 min, the supernatant was collected and transferred to a new tube, followed by incubation with GFP-Trap A beads (Chromotek, Planegg-Martinsried, Germany) at 4 °C for 90 min. The beads were collected and washed five times with lysis buffer by 2500 *g* centrifugation at 4 °C for 2 min. Finally, the beads in a 100-µl volume of lysis buffer were mixed with 25 µl 5 × loading buffer and boiled for 10 min to separate the proteins. The proteins were subsequently loaded on gels for sodium dodecyl sulfate-polyacrylamide gel electrophoresis (SDS-PAGE) and transferred to a polyvinylidene difluoride (PVDF) membrane. The membrane was blocked in 5% skim milk in TBST (20 mM Tris, 150 mM glycine, 0.1% Tween 20, pH7.5) for 2 h at RT, followed by incubation with anti-GFP (Abways, Shanghai, China), anti-mCherry (Sungenebiotech, Tianjin, China), or anti-HA monoclonal antibody (Abcam, Cambridge, UK, ab18181) at 4°C overnight. After washing by TBST for three times and incubation with goat-anti mouse IgG (Abways, Shanghai, China) secondary antibody for 1h, the blots were detected with ECL substrate kit (GE Healthcare, RPN2235).

Pull-down assay

The coding region of $RE02^{LRR}$ and $RLP23^{LRR}$ were cloned into pGEX-4T-1 vector (Amersham, Piscataway, NJ, USA) and mobilized in *E. coli* strain BL21(DE3) to produce GST-tagged proteins. Protein expressions were induced as described above. Supernatants containing GST-$RE02^{LRR}$ or GST-$RLP23^{LRR}$ fusion proteins were separately mixed with purified His-tagged VmE02 protein, and were then incubated with Glutathione Agarose (Thermo Scientific, Waltham, MA, USA) for 1 h at 4°C. The beads were collected by centrifugation and washed three times with equilibration buffer (50mM Tris, 150mM NaCl, pH 8.0). Protein samples eluted from the beads were subsequently subjected to western blotting analysis with anti-GST (Abways, Shanghai, China), and anti-HA antibodies (Abways, Shanghai, China).

Bioinformatics and data analysis

The signal peptide was predicted using the SignalP 5.0 server

(http://www.cbs.dtu.dk/services/SignalP/). The leucine-rich repeat domains were predicted with LRRfinder (http://www.lrrfinder.com/). Homologous sequences of RE02 were obtained from NCBI database by BLAST_P searches (https://blast.ncbi.nlm.nih.gov/Blast.cgi). VmE02 homologues in *P. capsici* and *S. sclerotiorum* can be respectively found in *P. capsici* reference genome (https://genome.jgi.doe.gov/Phyca11/Phyca11.home.html) and NCBI database. Phylogenetic maximum-likelihood dendrograms were constructed using MEGA 7 (Kumar *et al.*, 2016) and displayed by Evolview (Subramanian *et al.*, 2019). The data were analyzed with the online tool VassarStats (http://www.vassarstats.net/).

Results

RE02 is essential for VmE02 PAMP-triggered cell death

Most of the PRRs characterized thus far dynamically complex with co-receptors BAK1 or SOBIR1 to initiate signaling activation. Specially, SOBIR1 is required for the RLP-type PRRs as a signaling partner (Liebrand *et al.*, 2013; Liebrand *et al.*, 2014). Considering that VmE02-induced cell death in *Nicotiana benthamiana* is SOBIR1-depedent (Nie *et al.*, 2019), we speculated the PRR(s) for VmE02 is most likely to be an RLP. Therefore, we determined to knock down the RLP-encoding genes of *N. benthamiana* using virus-induced gene silencing (VIGS) to isolate the candidate PRRs for VmE02.

A total of 86 RLPs were identified in *N. benthamiana* genome (Wang *et al.*, 2018). Given that the typical PRRs are secreted and contain large ectodomains for ligand detection, we analyzed signal peptides and LRR domains for these RLPs. Finally, we focused on 29 RLPs that were individually predicated to contain a signal peptide and >10 LRR domains, and 21 silencing constructs were correspondingly designed (Table S3). These 21 independent RLP-silenced *N. benthamiana* plants were obtained and most of them showed no apparent alterations in growth or morphology (Fig. S1). To analyze the function of these *RLP* genes in VmE02-mediated responses, VmE02 was transiently expressed in these RLP-silenced plants. As a result, VmE02-induced cell death is greatly impaired in the T34-silencing line (Niben101Scf03240g00007.1), but not apparently affected in other plants (Fig. S2). Hereafter, we designated T34-targeted RLP as RE02

(Response to VmE02), and defined T34 as TRV2:*RE02-1*. To avoid potential off-target effects, another silencing construct TRV2:*RE02-2* targeted for *RE02* gene silencing was generated (Table S4). Neither of the two silencing constructs caused obvious growth alterations to *N. benthamiana* plants (Fig. S3). Transient expression analysis showed that, VmE02-induced cell death was almost abolished in both TRV2:*RE02-1* and TRV2:*RE02-2* silencing lines, compared with TRV2:*GFP*-treated control plants (Fig. 1a,b). In contrast, silencing of *RE02* showed no influence on INF1-triggered cell death, indicating that RE02 might specifically mediate VmE02 perception.

To further confirm RE02 response to VmE02, a cell death-complementation assay was performed in *RE02*-silenced plants using agroinfiltration. It showed that, VmE02-induced cell death could be successfully saved by co-expression with RE02, but not GFP or *Arabidopsis* RLP23 controls (Figs. 1c, S4). To be noted, RE02 *per se* showed no cell death-inducing activity in *N. benthamiana* (Fig. S5). Another, though being functional, C-terminal HA-tagged RE02 was not as efficient as RE02 alone to restore VmE02-induced cell death (Figs. 1c, S4), and GFP-tagged RE02 even failed to restore the cell death, suggesting that certain tags may variably interfere with RE02 bioactivity, similar to the cases of BAK1 and FLS2 (Ntoukakis *et al.*, 2011; Hurst *et al.*, 2018). Altogether, these results demonstrate that RE02 may participate in recognition of VmE02.

Since VmE02 homologues are widely spread in oomycete and fungi, some of which also elicit plant cell death (Nie *et al.*, 2019), we subsequently tested whether RE02 mediates their recognition similarly. Expectedly, VmE02 homologues from *Botrytis cinerea* (BC1G_05134), *Sclerotinia sclerotiorum* (sscle_06g048920), *Puccinia striiformis* f. sp. *tritici* (*Pst*) (PSTG_00149) and *Phytophthora parasitica* (PPTG_14297) all failed to triggered cell death when transiently expressed in *RE02*-silenced *N. benthamiana* (Fig. 1d), indicating that RE02 may participate in perception of VmE02 homologues from different pathogens.

RE02 mediates VmE02-triggered immune responses

To test whether RE02 mediates VmE02-induced defense responses, we measured VmE02-induced ROS burst and expression of PAMP-induced genes. It was shown that, VmE02-induced ROS was considerably attenuated in TRV2:*RE02*-treated *N. benthamiana* plants,

in contrast with plants treated with TRV2:*GFP* (Fig. 2a,b). However, *RE02*-silenced *N. benthamiana* showed no apparent influence on ROS production elicited by flg22 (Fig. S6), indicating the specificity of RE02 response to VmE02. To further confirm the capacity of RE02 to confer VmE02 sensitivity, we overexpressed RE02 in *N. benthamiana*, with RLP23 and NbCORE as controls. To eliminate potential complications from epitope tags (Figs. 1c, S4), these PRRs were equally expressed without any tag. As was shown, overexpression of RE02 but not RLP23 or NbCORE markedly promoted VmE02-triggered ROS production (Fig. 2c,d). Additionally, the transcript accumulation of PAMP-induced genes, including *PTI5*, *Acre31* and *CYP71D20* were greatly compromised in *RE02*-silenced plants after VmE02 treatment (Fig. 2e). These results collectively demonstrate that RE02 mediates VmE02-triggered immune responses.

RE02 directly binds to VmE02 with high affinity

To verify whether RE02 can associate with VmE02, C-terminal mCherry-tagged VmE02 and GFP-tagged RE02 were generated to perform a co-immunoprecipitation (Co-IP) assay in *N. benthamiana*. As was shown in Fig. 3a, RE02 but not RLP23 successfully coimmunoprecipitated with VmE02. In contrast, we failed to observe an interaction between RE02 and INF1 elicitin, suggesting RE02 specifically associates with VmE02 *in planta*. During western blotting analysis, to be noted, RE02 can only be detected after GFP-immunoprecipitation but not in total protein extracts (Fig. 3a). This may be due to receptor degradation and accordingly the low protein levels as seen in many other cases (Beck *et al.*, 2012).

In order to confirm RE02-VmE02 association and investigate their binding capacity, an *in vitro* pull-down and microscale thermophoresis (MST) assays were further performed. As was shown in Fig. 3b, the extracellular LRR domains of RE02 ($RE02^{LRR}$), but not that of RLP23 ($RLP23^{LRR}$) specifically copurified with VmE02. Furthermore, it also revealed a strong interaction between $RE02^{LRR}$ and VmE02 by MST analysis, with a dissociation constant (K_d) of 1.77±0.67 μM (Figs. 3c, S7). Thus, these data above indicate RE02 directly binds to VmE02 with high affinity.

RE02 forms a complex with BAK1 and SOBIR1

Since the co-receptors BAK1 and SOBIR1 usually function as PRR partners (Heese *et al.*, 2007; Liebrand *et al.*, 2013; Liebrand *et al.*, 2014), we next tested whether they associate with RE02. In the test to verify the interaction between RE02 and SOBIR1 by Co-IP, we found that RE02 continuously interacted with SOBIR1, regardless of treatment with VmE02 ligand or csp22 peptide (Fig. 4a). In contrast, the RLK NbCORE failed to interact with SOBIR1. This result is consistent with the previous reports that RLPs and SOBIR1 constitutively associate with each other (Gust & Felix, 2014; Wan *et al.*, 2019). Notably, we also observed a moderate interaction between RE02 and BAK1 even in the absence of ligands (Fig. 4b). However, RE02-BAK1 interaction was apparently enhanced upon VmE02 treatment, indicating BAK1 was recruited by RE02 in a ligand-sensitive manner. As a control, the interaction between NbCORE and BAK1 was only obviously detected when treated with the csp22 ligand but not VmE02 protein, consistent with a previous report (Wang *et al.*, 2016). It is worth mentioning that, csp22 peptide treatment also increased RE02-BAK1 interaction (Fig. 4B), indicating that RE02 recruitment of BAK1 is not ligand-specific.

BAK1 and SOBIR1 are essential for VmE02 immune responses

Considering the receptor complex of RE02-BAK1-SOBIR1, we next accessed the potential role of BAK1 and SOBIR1 in VmE02-triggered immune responses. For this, *BAK1*- and *SOBIR1*-silenced *N. benthamiana* plants were generated and tested for VmE02 responses. It was shown that, VmE02-triggered cell death was almost abolished in both *BAK1*- and *SOBIR1*-silenced plants (Fig. S8), which is consistent with our previous report (Nie *et al.*, 2019). In line with this, VmE02-incuded ROS production and the transcript accumulation of PAMP-induced genes (*PTI5*, *Acre31* and *CYP71D20*) were markedly compromised (Fig. 4c-f). These results demonstrated that BAK1 and SOBIR1 function as crucial components for VmE02-triggered immune responses.

RE02 regulates plant resistance against filamentous pathogens

PAMP perception frequently leads to plant resistance against multiple microbes. As VmE02 homologues are widely distributed in oomycetes and fungi, we then evaluated whether RE02 plays a role in plant resistance to such pathogens as *Phytophthora capsici* and *Sclerotinia sclerotiorum*. It showed that, *RE02*-silenced *N. benthamiana* plants displayed increased susceptibility to the oomycete *P. capsici* when compared with plants treated with TRV2:*GFP* (Fig. 5a). Analysis of relative biomass using quantitative polymerase chain reaction (qPCR) further confirmed this result, in which a notable increase of *P. capsici* biomass in *RE02*-silenced *N. benthamiana* was detected (Fig. 5b). Consistently, we found that silencing of *RE02* also promoted the disease severity of *S. sclerotiorum* (Fig. 5c). Disease-associated lesions caused by *S. sclerotiorum* were apparently larger in leaves targeted for *RE02* silencing (Fig. 5d). To further confirm RE02 contribution to plant resistance, we overexpressed RE02 (without any tag) in *N. benthamiana*. As expected, a decreased infection for both *P. capsici* and *S. sclerotiorum* could be observed in leaves expressing RE02, compared with those expressing GFP control (Fig. S9). Moreover, we found that the transcript levels of *PR1* and *PR4* were apparently reduced in *RE02*-silenced plants, suggesting RE02 positively regulates plant immunity (Fig. 5e). Altogether, these results illustrated that RE02 contributes to plant resistance against filamentous phytopathogens.

RE02 is identical to NbCSPR that exhibits csp22 binding affinity

Apart from *N. benthamiana*, VmE02 is also detected by several other plant species including *Arabidopsis thaliana*, tomato (*Solanum lycopersicum*), pepper (*Capsicum annuum*) and its apple host (*Malus domestica*) (Nie *et al.*, 2019). To determine whether there exists RE02 homologues in other plants, the sequence of RE02 was queried against NCBI database by BLAST_P searches. It showed that, RE02 close homologues are exclusively distributed in Solanaceae plants, particularly the *Nicotiana* species, such as *N. sylvestris*, *N. tomentosiformis* and *N. tabacum*, with 95.4%, 92.6%, and 93.8% sequence identity, respectively (Fig. 6a, Table S5). Intriguingly, no obvious homologues were found in *A. thaliana*, *S. lycopersicum*, *C. annuum*, or *M. domestica*, in which the most closely related sequences separately share 30.4%, 50.6%, 49.5% and 45.4% identity with RE02 (Table S5).

In *N. benthamiana*, RXEG1 and NbCSPR were two of the few characterized PRRs to date, which receptively mediates perception of *Phytophthora* XEG1 and bacterial cold-shock protein (csp22) (Saur *et al.*, 2016; Wang *et al.*, 2018). As reported, NbCSPR is a Solanaceae-specific RLP (Saur *et al.*, 2016), which is similar to the distribution feature of RE02. This prompt us to compare their sequences. Strikingly, these two sequences were shown to be totally identical (Fig. S10), indicating that they represent the same PRR. As indicated above, RE02 (hereafter also known as NbCSPR) displayed a high affinity for VmE02 (Fig. 3b). However, the affinity between RE02 and csp22 is unknown, though they were revealed to interact with each other (Saur *et al.*, 2016). For this, RE02 binding capacity for csp22 was tested by MST analysis. As shown in Fig. 6b, an obvious interaction between $RE02^{LRR}$ and csp22 was observed, with a dissociation constant (K_d) of 296.2±45.7 μM, while no binding affinity was detected between $RE02^{LRR}$ and Flg22 peptide. It is notable that, RE02 binding affinity for csp22 is roughly 160-fold lower than that measured for VmE02 under the same conditions (K_d =1.77±0.67 μM) (Fig. 3b). Taken together, these results demonstrate that RE02 is identical to NbCSPR and exhibits binding affinity for csp22.

Discussion

With a growing number of extracellular PAMPs being identified, the PRRs for their recognition are poorly characterized. In this study, using both genetics and biochemistry analysis, we found the receptor-like protein RE02 in *N. benthamiana* exhibits features for a receptor of the PAMP VmE02. These include sufficient responsiveness to VmE02-induced cell death, VmE02-triggererd immune responses, and direct combination to VmE02 with high affinity.

The RLP-type PRRs lack typical cytoplasmic signaling domains, for which, they were proposed to form a complex with SOBIR1 as a partner and constitute equivalent two-component RLKs (Gust & Felix, 2014). RLP23 and RLP42 in *Arabidopsis*, Cfs and Ve1 in tomato, ELR in potato, and RXEG1 in *N. benthamiana*, all constitutively associate with SOBIR1 for downstream responses (Liebrand et at., 2013; Albert *et al.*, 2015; Zhang *et al.*, 2014; Domazakis *et al.*, 2018; Wang *et al.*, 2018). Consistently, in this study, we found that RE02 formed a complex with SOBIR1 independent of ligand treatment (Fig. 4a). As another adaptor, BAK1 also associates with

a variety of PRRs, however, the interactions between them are quite flexible. Several PRRs, like LYK5, CERK1, and LORE do not require BAK1 for PAMP recognition (Miya *et al.*, 2007; Cao *et al.*, 2014; Ranf *et al.*, 2015); the RLK-type PRRs like FLS2, EFR, CORE, and the RLP-type PRRs such as RLP23 and Cf-4 only combine with BAK1 in the presence of their cognate ligands (Heese *et al.*, 2007; Roux *et al.*, 2011; Albert *et al.*, 2015; Postma *et al.*, 2016; Wang *et al.*, 2016); the RLP ELR and RXEG1 constitutively associate with BAK1, whereas, ligand treatment enhanced their interactions (Du *et al.*, 2015; Domazakis *et al.*, 2018; Wang *et al.*, 2018). In this study, similar to ELR and RXEG1, RE02 was shown to associate with BAK1 in the absence of VmE02, while VmE02 treatment obviously increased RE02-BAK1 interaction (Fig. 4b), suggesting that VmE02 could help to recruit BAK1 and stabilize their combination. Our further data revealed that both BAK1 and SOBIR1 were indispensable components for VmE02-induced immune responses (Fig. 4c-e). Therefore, RE02, SOBIR1 and BAK1 constitute a tri-partite complex to confer plant responsiveness to VmE02.

We previously found that VmE02 induces cell death response in multiple plant species including *A. thaliana*, *S. lycopersicum*, and its cognate host *M. domestica* (Nie *et al.*, 2019). However, in each of these plants, we were unable to identify a clear sequence homolog of RE02, whose most related sequences mainly distribute in some *Nicotiana* species (Fig. 6a, Table S5). In fact, with exception for FLS2, the vast majority of plant PRRs display a genus- or subgenus-specific occurrence, particularly the RLP-type PRRs (Wan *et al.*, 2019; Albert *et al.*, 2020). It is possible that *Arabidopsis*, tomato, and apple have evolved different PRRs to mediate VmE02 responses, similar to the case of chitin perceptions by different plants. In *Oryza sativa*, the RLP OsCEBiP is the main receptor for binding of chitin elicitor (Ito *et al.*, 1997; Kaku *et al.*, 2006). However, in *Arabidopsis*, chitin is mainly bind by LYK5, an RLK-type PRR (Cao *et al.*, 2014). Alternatively, considering the diverse conserved regions among VmE02 and its homologues (Nie *et al.*, 2019), VmE02 may carry divergent epitopes that are recognized by distinct PRRs. To better understand how VmE02 is recognized, receptors for its recognition in other plants should be investigated in future.

Thus far, apart from RXEG1 and NbCSPR which respectively mediate perception of

Phytophthora XEG1 and bacterial cold-shock protein (csp22) (Saur *et al.*, 2016; Wang *et al.*, 2018), few PRRs were characterized in the model plant *N. benthamiana*. We also failed to match any known PRRs in *N. benthamiana* genome during BLAST_P queries. Nonetheless, the distribution feature of RE02 is quite similar to that of NbCSPR, whose homologues exclusively exist in limited Solanaceae plants as well (Saur *et al.*, 2016). This stimulated us to compare their protein sequences, and surprisingly, we found the two RLPs represent the same PRR (Fig. S10). This unexpected finding suggests that RE02 (also known as NbCSPR) is likely to participate in recognition of both eukaryotic and prokaryotic PAMPs. In line with this, we found that ligand treatment by either VmE02 or csp22 promoted RE02-BAK1 association (Fig. 4b). Additionally, RE02 (NbCSPR) was revealed to associate with csp22 peptide (Saur *et al.*, 2016), and in this study we found it interacted with VmE02 as well (Fig. 3a-b). Most importantly, our MST assays revealed that RE02 displayed binding affinity for both VmE02 and csp22 (Figs 3b, 6b), further confirming RE02 functions as a PRR for both of these two PAMPs. This result is reminiscent of several reported PRRs including the RLK CERK1 in *Arabidopsis*, and the RLPs LYP4 and LYP6 in rice, all of which mediate recognition of both fungal chitin and bacterial peptidoglycan (Miya *et al.*, 2007; Willmann *et al.*, 2011; *Liu et al.*, 2012).

Interestingly, csp22 was also demonstrated to be detected by Solanaceae CORE, an RLK-type receptor with high affinity for csp22 (Wang *et al.*, 2016). In this study, we also showed that csp22 treatment enhanced the interaction between BAK1 and NbCORE (Fig. 4b), a functional homologue of CORE in *N. benthamiana*, confirming the role of CORE in csp22 perception. To be noted, it was revealed that CORE but not RE02 confers sufficient plant responsiveness to csp22 (Wang *et al.*, 2016). We also obtained similar results showing that NbCORE but not RE02 notably promoted csp22-elicited ROS burst when transiently expressed in young *N. benthamiana* plants (Fig. S11). This discrepancy may attribute to the dramatical affinity difference between CORE and RE02 for csp22 peptide. As reported, CORE shows a quite strong affinity for csp22 (K_d ~60 nM) (Wang *et al.*, 2016), however, RE02 exhibited a much weaker affinity for the same peptide (K_d =296.2±45.7 μM) (Fig. 6b). Therefore, CORE is probably the main receptor for csp22. In addition, since RE02 showed a high affinity for VmE02 protein (K_d =1.77±0.67 μM) (Fig. 3b), it is most

likely to function as the main receptor for the PAMP VmE02.

A variety of oomycete and fungal pathogens carry VmE02 homologues with cell death-inducing activity, and VmE02 treatment enhances plant resistance to filamentous phytopathogens (Nie *et al.*, 2019). In this study, RE02 was also shown to mediate *N. benthamiana* resistance to both the oomycete *P. capsici* and the fungus *S. sclerotiorum* (Fig. 5a-d). Moreover, RE02 (NbCSPR) was demonstrated to confer plant resistance to bacterial pathogens as well (Saur *et al.*, 2016). In recent years, multiple researches have showed that individual or stacked transfer of PRRs contribute to crop disease resistance quantitatively and durably (Dangle *et al.*, 2013; Albert *et al.*, 2015; Du *et al.*, 2015). Therefore, RE02 represents a promising candidate PRR for engineering crop immunity. Particularly, since the monocot wheat exhibits no response to VmE02 (Nie *et al.*, 2019), it remains to be explored whether transfer of RE02 in wheat would confer VmE02 sensitivity and plant resistance. If it is the case, RE02 may be useful for building wheat resistance against the devastating fungal pathogens such as rust fungi and *Fusarium graminearum*, both of which carry homologues of VmE02 (Nie *et al.*, 2019).

Genetics is considered as one of the most powerful methods to identify PRRs for multiple PAMPs (Boutrot & Zipfel, 2017). Genome-wide silencing of LRR-like genes in *N. benthamiana* was recently developed as a novel reverse-genetic method to successfully identified RXEG1, which mediates glycoside hydrolase 12 detection (Wang *et al.*, 2018). In this study, we adopted a modified approach by silencing the RLPs with typical PRR features, and identified RE02 as a recognition receptor for VmE02, further confirming virus-induced gene silencing (VIGS) as an efficient approach for PRRs identification in the model plant *N. benthamiana*.

Acknowledgements

We thank Daolong Dou at Nanjing Agricultural University, Huiquan Liu at Northwest A&F University, and Xuli Wang at Chinese Academy of Agricultural Sciences for helpful suggestions on this manuscript. This work was supported by National Natural Science Foundation of China (31671982), and National Natural Science Foundation-Xinjiang Joint Foundation of China (U1903206).

Author contributions

L.H., J.-M.Z. and J.N. designed and conceived the research. J.N., W.Z., J.L., and N.T. performed the experiments. J.N., and L.H. analyzed the data. J.N., and L.H. wrote the manuscript. All authors discussed the results and commented on the manuscript before submission.

References

Akira S, Uematsu S, Takeuchi O. 2006. Pathogen recognition and innate immunity. *Cell* **124**(4): 783-801.

Albert I, Böhm H, Albert M, Feiler CE, Imkampe J, Wallmeroth N, Brancato C, Raaymakers TM, Oome S, Zhang H. 2015. An RLP23–SOBIR1–BAK1 complex mediates NLP-triggered immunity. *Nature Plants* **1**(10): 1-9.

Albert I, Hua C, Nürnberger T, Pruitt RN, Zhang L. 2020. Surface sensor systems in plant immunity. *Plant physiology* **182**(4): 1582.

Beck M, Heard W, Mbengue M, Robatzek S. 2012. The INs and OUTs of pattern recognition receptors at the cell surface. *Current opinion in plant biology* **15**(4): 367-374.

Boutrot F, Zipfel C. 2017. Function, discovery, and exploitation of plant pattern recognition receptors for broad-spectrum disease resistance. *Annual review of phytopathology* **55**: 257-286.

Cao Y, Liang Y, Tanaka K, Nguyen CT, Jedrzejczak RP, Joachimiak A, Stacey G. 2014. The kinase LYK5 is a major chitin receptor in *Arabidopsis* and forms a chitin-induced complex with related kinase CERK1. *elife* **3**: e03766.

Chinchilla D, Bauer Z, Regenass M, Boller T, Felix G. 2006. The *Arabidopsis* receptor kinase FLS2 binds flg22 and determines the specificity of flagellin perception. *The Plant Cell* **18**(2): 465-476.

Couto D, Zipfel C. 2016. Regulation of pattern recognition receptor signalling in plants. *Nature Reviews Immunology* **16**(9): 537.

Dangl JL, Horvath DM, Staskawicz BJ. 2013. Pivoting the plant immune system from

dissection to deployment. *Science* **341**(6147): 746-751.

de Jonge R, van Esse HP, Maruthachalam K, Bolton MD, Santhanam P, Saber MK, Zhang Z, Usami T, Lievens B, Subbarao KV. 2012. Tomato immune receptor Ve1 recognizes effector of multiple fungal pathogens uncovered by genome and RNA sequencing. *Proceedings of the National Academy of Sciences* **109**(13): 5110-5115.

de Wit PJ. 2016. *Cladosporium fulvum* effectors: weapons in the arms race with tomato. *Annual review of phytopathology* **54**: 1-23.

Domazakis E, Wouters D, Visser RG, Kamoun S, Joosten MH, Vleeshouwers VG. 2018. The ELR-SOBIR1 complex functions as a two-component receptor-like kinase to mount defense against *Phytophthora infestans*. *Molecular Plant-Microbe Interactions* **31**(8): 795-802.

Du J, Verzaux E, Chaparro-Garcia A, Bijsterbosch G, Keizer LP, Zhou J, Liebrand TW, Xie C, Govers F, Robatzek S. 2015. Elicitin recognition confers enhanced resistance to *Phytophthora infestans* in potato. *Nature Plants* **1**(4): 1-5.

Fritz-Laylin LK, Krishnamurthy N, Tör M, Sjölander KV, Jones JD. 2005. Phylogenomic analysis of the receptor-like proteins of rice and *Arabidopsis*. *Plant physiology* **138**(2): 611-623.

Gómez-Gómez L, Boller T. 2000. FLS2: an LRR receptor–like kinase involved in the perception of the bacterial elicitor flagellin in *Arabidopsis*. *Molecular cell* **5**(6): 1003-1011.

Gust AA, Felix G. 2014. Receptor like proteins associate with SOBIR1-type of adaptors to form bimolecular receptor kinases. *Current opinion in plant biology* **21**: 104-111.

Heese A, Hann DR, Gimenez-Ibanez S, Jones AM, He K, Li J, Schroeder JI, Peck SC, Rathjen JP. 2007. The receptor-like kinase SERK3/BAK1 is a central regulator of innate immunity in plants. *Proceedings of the National Academy of Sciences* **104**(29): 12217-12222.

Hind SR, Strickler SR, Boyle PC, Dunham DM, Bao Z, O'Doherty IM, Baccile JA, Hoki JS, Viox EG, Clarke CR. 2016. Tomato receptor FLAGELLIN-SENSING 3 binds flgII-28 and activates the plant immune system. *Nature Plants* **2**(9): 1-8.

Hurst CH, Turnbull D, Myles SM, Leslie K, Keinath NF, Hemsley PA. 2018. Variable effects of C-terminal fusions on FLS2 function: Not all epitope tags are created equal. *Plant physiology* **177**(2): 522-531.

Ito Y, Kaku H, Shibuya N. 1997. Identification of a high-affinity binding protein for N-acetylchitooligosaccharide elicitor in the plasma membrane of suspension-cultured rice cells by affinity labeling. *The Plant Journal* **12**(2): 347-356.

Jehle AK, Lipschis M, Albert M, Fallahzadeh-Mamaghani V, Fürst U, Mueller K, Felix G. 2013. The receptor-like protein ReMAX of *Arabidopsis* detects the microbe-associated molecular pattern eMax from *Xanthomonas*. *The Plant Cell* **25**(6): 2330-2340.

Kaku H, Nishizawa Y, Ishii-Minami N, Akimoto-Tomiyama C, Dohmae N, Takio K, Minami E, Shibuya N. 2006. Plant cells recognize chitin fragments for defense signaling through a plasma membrane receptor. *Proceedings of the National Academy of Sciences* **103**(29): 11086-11091.

Kumar S, Stecher G, Tamura K. 2016. MEGA7: molecular evolutionary genetics analysis version 7.0 for bigger datasets. *Molecular biology and evolution* **33**(7): 1870-1874.

Lacombe S, Rougon-Cardoso A, Sherwood E, Peeters N, Dahlbeck D, Van Esse HP, Smoker M, Rallapalli G, Thomma BP, Staskawicz B. 2010. Interfamily transfer of a plant pattern-recognition receptor confers broad-spectrum bacterial resistance. *Nature biotechnology* **28**(4): 365-369.

Liebrand TW, van den Berg GC, Zhang Z, Smit P, Cordewener JH, America AH, Sklenar J, Jones AM, Tameling WI, Robatzek S. 2013. Receptor-like kinase SOBIR1/EVR interacts with receptor-like proteins in plant immunity against fungal infection. *Proceedings of the National Academy of Sciences* **110**(24): 10010-10015.

Liebrand TW, van den Burg HA, Joosten MH. 2014. Two for all: receptor-associated kinases SOBIR1 and BAK1. *Trends in plant science* **19**(2): 123-132.

Liu B, Li J-F, Ao Y, Qu J, Li Z, Su J, Zhang Y, Liu J, Feng D, Qi K. 2012. Lysin motif–containing proteins LYP4 and LYP6 play dual roles in peptidoglycan and chitin perception in rice innate immunity. *The Plant Cell* **24**(8): 3406-3419.

Livak KJ, Schmittgen TD. 2001. Analysis of relative gene expression data using real-time quantitative PCR and the $2^{-\Delta\Delta CT}$ method. *Methods* **25**(4): 402-408.

Miya A, Albert P, Shinya T, Desaki Y, Ichimura K, Shirasu K, Narusaka Y, Kawakami N, Kaku H, Shibuya N. 2007. CERK1, a LysM receptor kinase, is essential for chitin elicitor signaling in *Arabidopsis*. *Proceedings of the National Academy of Sciences* **104**(49): 19613-19618.

Mott GA, Thakur S, Smakowska E, Wang PW, Belkhadir Y, Desveaux D, Guttman DS. 2016. Genomic screens identify a new phytobacterial microbe-associated molecular pattern and the cognate *Arabidopsis* receptor-like kinase that mediates its immune elicitation. *Genome biology* **17**(1): 98.

Nie J, Yin Z, Li Z, Wu Y, Huang L. 2019. A small cysteine-rich protein from two kingdoms of microbes is recognized as a novel pathogen-associated molecular pattern. *New Phytologist* **222**(2): 995-1011.

Ntoukakis V, Schwessinger B, Segonzac C, Zipfel C. 2011. Cautionary notes on the use of C-terminal BAK1 fusion proteins for functional studies. *The Plant Cell* **23**(11): 3871-3878.

Postma J, Liebrand TW, Bi G, Evrard A, Bye RR, Mbengue M, Kuhn H, Joosten MH, Robatzek S. 2016. Avr4 promotes Cf-4 receptor-like protein association with the BAK1/SERK3 receptor-like kinase to initiate receptor endocytosis and plant immunity. *New Phytologist* **210**(2): 627-642.

Pruitt RN, Schwessinger B, Joe A, Thomas N, Liu F, Albert M, Robinson MR, Chan LJG, Luu DD, Chen H. 2015. The rice immune receptor XA21 recognizes a tyrosine-sulfated protein from a Gram-negative bacterium. *Science Advances* **1**(6): e1500245.

Ranf S, Gisch N, Schäffer M, Illig T, Westphal L, Knirel YA, Sánchez-Carballo PM, Zähringer U, Hückelhoven R, Lee J. 2015. A lectin S-domain receptor kinase mediates lipopolysaccharide sensing in *Arabidopsis thaliana*. *Nature immunology* **16**(4): 426.

Ron M, Avni A. 2004. The receptor for the fungal elicitor ethylene-inducing xylanase is a member of a resistance-like gene family in tomato. *The Plant Cell* **16**(6): 1604-1615.

Roux M, Schwessinger B, Albrecht C, Chinchilla D, Jones A, Holton N, Malinovsky FG, Tör

M, de Vries S, Zipfel C. 2011. The *Arabidopsis* leucine-rich repeat receptor–like kinases BAK1/SERK3 and BKK1/SERK4 are required for innate immunity to hemibiotrophic and biotrophic pathogens. *The Plant Cell* **23**(6): 2440-2455.

Sang Y, Macho AP 2017. Analysis of PAMP-triggered ROS burst in plant immunity. In: Shan L, He P, eds. Plant Pattern Recognition Receptors. *Methods in Molecular Biology*. New York, NY: Humana Press, 143-153.

Saur IM, Kadota Y, Sklenar J, Holton NJ, Smakowska E, Belkhadir Y, Zipfel C, Rathjen JP. 2016. NbCSPR underlies age-dependent immune responses to bacterial cold shock protein in *Nicotiana benthamiana*. *Proceedings of the National Academy of Sciences* **113**(12): 3389-3394.

Shiu S-H, Karlowski WM, Pan R, Tzeng Y-H, Mayer KF, Li W-H. 2004. Comparative analysis of the receptor-like kinase family in Arabidopsis and rice. *The Plant Cell* **16**(5): 1220-1234.

Subramanian B, Gao S, Lercher MJ, Hu S, Chen W-H. 2019. Evolview v3: a webserver for visualization, annotation, and management of phylogenetic trees. *Nucleic acids research* **47**(W1): W270-W275.

Sun Y, Li L, Macho AP, Han Z, Hu Z, Zipfel C, Zhou J-M, Chai J. 2013. Structural basis for flg22-induced activation of the *Arabidopsis* FLS2-BAK1 immune complex. *Science* **342**(6158): 624-628.

Tang D, Wang G, Zhou J-M. 2017. Receptor kinases in plant-pathogen interactions: more than pattern recognition. *The Plant Cell* **29**(4): 618-637.

Wan W-L, Fröhlich K, Pruitt RN, Nürnberger T, Zhang L. 2019. Plant cell surface immune receptor complex signaling. *Current opinion in plant biology* **50**: 18-28.

Wang G, Ellendorff U, Kemp B, Mansfield JW, Forsyth A, Mitchell K, Bastas K, Liu C-M, Woods-Tör A, Zipfel C. 2008. A genome-wide functional investigation into the roles of receptor-like proteins in *Arabidopsis*. *Plant physiology* **147**(2): 503-517.

Wang L, Albert M, Einig E, Fürst U, Krust D, Felix G. 2016. The pattern-recognition receptor CORE of Solanaceae detects bacterial cold-shock protein. *Nature Plants* **2**(12): 16185.

Wang Y, Xu Y, Sun Y, Wang H, Qi J, Wan B, Ye W, Lin Y, Shao Y, Dong S. 2018. Leucine-rich repeat receptor-like gene screen reveals that *Nicotiana* RXEG1 regulates glycoside hydrolase 12 MAMP detection. *Nature communications* **9**(1): 1-12.

Willmann R, Lajunen HM, Erbs G, Newman M-A, Kolb D, Tsuda K, Katagiri F, Fliegmann J, Bono J-J, Cullimore JV. 2011. *Arabidopsis* lysin-motif proteins LYM1 LYM3 CERK1 mediate bacterial peptidoglycan sensing and immunity to bacterial infection. *Proceedings of the National Academy of Sciences* **108**(49): 19824-19829.

Wu J, Reca IB, Spinelli F, Lironi D, De Lorenzo G, Poltronieri P, Cervone F, Joosten MH, Ferrari S, Brutus A. 2019. An EFR-Cf-9 chimera confers enhanced resistance to bacterial pathogens by SOBIR1-and BAK1-dependent recognition of elf18. *Molecular plant pathology* **20**(6): 751-764.

Yamaguchi Y, Pearce G, Ryan CA. 2006. The cell surface leucine-rich repeat receptor for AtPep1, an endogenous peptide elicitor in Arabidopsis, is functional in transgenic tobacco cells. *Proceedings of the National Academy of Sciences* **103**(26): 10104-10109.

Yu X, Tang J, Wang Q, Ye W, Tao K, Duan S, Lu C, Yang X, Dong S, Zheng X. 2012. The RxLR effector Avh241 from *Phytophthora sojae* requires plasma membrane localization to induce plant cell death. *New Phytologist* **196**(1): 247-260.

Zhang L, Kars I, Essenstam B, Liebrand TW, Wagemakers L, Elberse J, Tagkalaki P, Tjoitang D, van den Ackerveken G, van Kan JA. 2014. Fungal endopolygalacturonases are recognized as microbe-associated molecular patterns by the *Arabidopsis* receptor-like protein RESPONSIVENESS TO BOTRYTIS POLYGALACTURONASES1. *Plant physiology* **164**(1): 352-364.

Zhang W, Fraiture M, Kolb D, Löffelhardt B, Desaki Y, Boutrot FF, Tör M, Zipfel C, Gust AA, Brunner F. 2013. *Arabidopsis* receptor-like protein30 and receptor-like kinase suppressor of BIR1-1/EVERSHED mediate innate immunity to necrotrophic fungi. *The Plant Cell* **25**(10): 4227-4241.

Zipfel C, Kunze G, Chinchilla D, Caniard A, Jones JD, Boller T, Felix G. 2006. Perception of the bacterial PAMP EF-Tu by the receptor EFR restricts *Agrobacterium*-mediated

transformation. *Cell* **125**(4): 749-760.

Figure legends

Fig. 1 RE02 mediates VmE02 PAMP-triggered cell death in *Nicotiana benthamiana*. (a) Representative leaves showing cell death induced by VmE02 or INF1 in TRV2:*GFP*- or TRV2:*RE02*-treated *N. benthamiana*. Infiltrated leaves (n = 6) were photographed five days post agroinfiltration (dpa). The experiment was performed at least three times with similar results. Immunoblot analysis of expressed proteins were performed with anti-mCherry antibody. Rubisco protein was stained with Ponceau S as a loading control. (b) Silencing efficiency of *RE02* determined by qRT-PCR analysis. Relative expression of *RE02* was normalized to *NbActin* and calibrated to the levels of TRV2:*GFP*-treated leaves (set as 1). Values represent means ± SE of three biological replicates. Differences were assessed by Student's *t*-test. ***, $P < 0.001$. (c) Representative leaves showing cell death induced by co-expression of VmE02 with RE02, RLP23, or GFP in TRV2:*GFP*- or TRV2:*RE02*-treated *N. benthamiana*. Infiltrated leaves (n = 6) were photographed 5 dpa. The experiment was performed at least three times with similar results. VmE02 protein expression was analyzed anti-mCherry antibody, and Rubisco protein was stained with Ponceau S as a loading control. (d) Representative leaves showing cell death induced by VmE02 homologues in TRV2:*GFP*- or TRV2:*RE02*-treated *N. benthamiana*. VmE02 homologues including PSTG_00149 from *Puccinia striiformis* f. sp. *tritici* (*Pst*), BC1G_05134 from *Botrytis cinerea*, sscle_06g048920 from *Sclerotinia sclerotiorum* and PPTG_14297 from *Phytophthora parasitica* were transiently expressed in *N. benthamiana*. The numbers from 1 to 6 refer to PSTG_00149, BC1G_05134, VmE02, PPTG_14297, sscle_06g048920 and INF1, respectively. Photographs for infiltrated leaves (n = 6) were taken 5 dpa. The experiment was performed at least three times with similar results. Protein accumulation of each protein was monitored with anti-mCherry antibody, and Rubisco protein was stained with Ponceau S as a loading control.

Fig. 2 RE02 mediates VmE02-triggered plant immune responses. (a, b) Oxidative burst in *GFP*- or *RE02*-silenced *Nicotiana benthamiana* treated with 1 μM VmE02. Values represent means ± SE

of eight biological replicates. Differences were assessed by Student's *t*-test. **, $P < 0.01$; ***, $P < 0.001$. The experiment was performed three times with similar results. (c, d) Oxidative burst in *RE02*-, *RLP23*-, or *NbCORE*-expressing *N. benthamiana* treated with 1 μM VmE02. RE02, RLP23 and NbCORE without any tag were transiently expressed in *N. benthamiana* using agroinfiltration individually. Values represent means ± SE of eight biological replicates. Differences were assessed by Student's *t*-test. *, $P < 0.05$; ***, $P < 0.001$. The experiment was performed three times with similar results. (e) Transcript accumulation of *PTI5*, *Acre31*, and *Cyp71D20* in *GFP*- or *RE02*-silenced *N. benthamiana* leaves 6 h post treatment with 500 nM VmE02. Transcript levels were determined by qRT-PCR. Relative expression of each gene was normalized to *NbActin* and calibrated to the levels of buffer-treated leaves (set as 1). Values represent means ± SE of three biological replicates. Differences were assessed by Student's *t*-test. *, $P < 0.05$; **, $P < 0.01$. The experiment was performed three times with similar results. RLU, relative luminescence units.

Fig. 3 RE02 directly binds to VmE02. (a) Association between RE02 and VmE02 *in planta*. *Nicotiana benthamiana* leaves co-expressing GFP-tagged RE02 or RLP23 and mCherry-tagged VmE02 or INF1 were collected 36 h post agroinfiltration (hpa), and co-immunoprecipitation (IP) was performed on proteins isolated from these samples. Proteins samples were subjected to western blotting using anti-GFP and anti-mCherry antibodies. Rubisco protein from input samples was stained with Ponceau S as a loading control. (b) Interaction between RE02 and VmE02 *in vitro*. GST-tagged $RE02^{LRR}$ (RE02 LRR domains) and His-tagged VmE02 were expressed in *Escherichia coli*, and the protein-protein interaction was tested by GST pull-down assay. GST-tagged $RLP23^{LRR}$ (RLP23 LRR domains) was used as a control. Proteins samples were subjected to western blotting analysis using anti-GST and anti-His antibodies. (c) Determination of RE02 binding affinity for VmE02 by microscale thermophoresis (MST) analysis. Labelled $RE02^{LRR}$ or $RLP23^{LRR}$ was mixed with gradient dilution of VmE02 recombinant protein. The data were analyzed by plotting the concentration of VmE02 against the changes in fluorescence of labeled $RE02^{LRR}$ or $RLP23^{LRR}$ using a non-linear fit. Values represent means ± SE of three

technical replicates. This experiment was repeated three times with similar results.

Fig. 4 RE02 associates with BAK1 and SOBIR1 for recognition of VmE02. (a, b) Interactions of RE02 with SOBIR1 and BAK1 *in planta*. *Nicotiana benthamiana* leaves co-expressing HA-tagged SOBIR1 or BAK1 and GFP-tagged RE02 or NbCORE were collected 36 hpa after treatment with 1 μM VmE02 or csp22 for 20 min. Co-IP was performed on proteins isolated from these samples. Proteins samples were subjected to western blotting using anti-GFP and anti-HA antibodies. Rubisco protein from input samples was stained with Ponceau S as a loading control. (c, d) Oxidative burst in *BAK1*- or *SOBIR1*-silenced *N. benthamiana* treated with 1 μM VmE02. Values represent means ± SE of eight biological replicates. Differences were assessed by Student's *t*-test. **, $P < 0.01$; ***, $P < 0.001$. The experiment was performed three times with similar results. (e) Silencing efficiency of *BAK1* and *SOBIR1* determined by qRT-PCR analysis. Relative expression of *BAK1* or *SOBIR1* was normalized to *NbActin* and calibrated to the levels of TRV2:*GFP*-treated leaves (set as 1). Values represent means ± SE of three biological replicates. Differences were assessed by Student's *t*-test. *, $P < 0.05$; **, $P < 0.01$. (f) Transcript accumulation of *PTI5*, *Acre31*, and *Cyp71D20* in *GFP*-, *BAK1*, or *SOBIR1*-silenced *N. benthamiana* leaves 6 h post treatment with 500 nM VmE02. Transcript levels were determined by qRT-PCR. Relative expression of each gene was normalized to *NbActin* and calibrated to the levels of buffer-treated leaves (set as 1). Values represent means ± SE of three biological replicates. Differences were assessed by Student's *t*-test. *, $P < 0.05$; **, $P < 0.01$. The experiment was performed three times with similar results. RLU, relative luminescence units.

Phytophthora capsici and *Sclerotinia sclerotiorum*

Fig. 5 RE02 regulates *Nicotiana benthamiana* resistance against *Phytophthora capsici* and *Sclerotinia sclerotiorum*. (a) Representative leaves showing disease lesions of *GFP*- or *RE02*-silenced *N. benthamiana* infected with *P. capsici*. The leaves (n = 6) were inoculated with *P. capsici* fresh mycelial plugs and photographed 36 h post inoculation (hpi). The experiment was repeated three times with similar results. (b) Quantification of *P. capsici* infection by qRT-PCR to measure the ratios of *P. capsici* to *N. benthamiana* DNA. Values represent means ± SE of three

biological replicates. Differences were assessed by Student's *t*-test. **, $P < 0.01$. (c) Representative leaves showing disease lesions of *GFP*- or *RE02*-silenced *N. benthamiana* infected with *S. sclerotiorum*. The leaves (n = 6) were inoculated with *S. sclerotiorum* fresh mycelial plugs and photographed 24 hpi. The experiment was repeated three times with similar results. (d) Lesion diameters of *N. benthamiana* leaves infected by *S. sclerotiorum*. Values represent means ± SE of six biological replicates. Differences were assessed by Student's *t*-test. **, $P < 0.01$; ***, $P < 0.001$. (e) Transcript accumulation of *PR1* and *PR4* in *RE02*-silenced *N. benthamiana*. Relative expression of both genes were normalized to *NbActin* and calibrated to the levels of TRV2:*GFP*-treated leaves (set as 1). Values represent means ± SE of three biological replicates. Differences were assessed by Student's *t*-test. **, $P < 0.01$; ***, $P < 0.001$. The experiment was repeated three times with similar results.

Fig. 6 RE02 exhibits binding affinity for csp22. (a) Phylogenetic analysis of RE02 and closely related proteins in different plants. Bootstrap percentage support for each branch is indicated. The red branches show the subgroup for RE02 close homologues. RE02 is marked by a red circle. (b) Determination of RE02 binding affinity for csp22 using microscale thermophoresis (MST) analysis. Labelled $RE02^{LRR}$ was mixed with gradient dilution of csp22 or Flg22. The data were analyzed by plotting the concentration of csp22 or Flg22 against the changes in fluorescence of labeled $RE02^{LRR}$ using a non-linear fit. Values represent means ± SE of three technical replicates. This experiment was repeated three times with similar results.

Supporting information

Fig. S1 Morphology of *N. benthamiana* plants treated with *RLP*-silencing constructs.

Fig. S2 Representative leaves showing cell death induced by VmE02 or INF1 in *N. benthamiana* plants treated with *RLP*-silencing constructs.

Fig. S3 Morphology of *N. benthamiana* plants treated with *RE02*-silencing constructs.

Fig. S4 Representative leaves showing cell death induced by co-expression of VmE02 with epitopes-tagged RE02 or RLP23 in TRV2:*GFP*- or TRV2:*RE02*-treated *N. benthamiana*.

Fig. S5 Transient expression of RE02 does not induce cell death in *N. benthamiana*.

Fig. S6 Silencing of *RE02* shows no apparent influence on Flg22-induced oxidative burst in *N. benthamiana*.

Fig. S7 Western blotting analysis of recombinant $RE02^{LRR}$, $RLP23^{LRR}$ and VmE02 proteins used for microscale thermophoresis (MST) analysis.

Fig. S8 Representative leaves showing cell death induced by VmE02 in *BAK1*- or *SOBIR1*-silenced *N. benthamiana*.

Fig. S9 Overexpression of RE02 enhances *N. benthamiana* resistance to *P. capsici* and *S. sclerotiorum*.

Fig. S10 Protein sequence alignment of RE02 with NbCSPR using ClustalW.

Fig. S11 Overexpression of NbCORE in young *N. benthamiana* promoted csp22-induced oxidative burst.

Table S1 Primers used in this study.

Table S2 VmE02 homologues in *Phytophthora capsici* and *Sclerotinia sclerotiorum*.

Table S3 Information of *RLP*-silencing constructs in this study.

Table S4 Fragments for *RE02* gene silencing.

Table S5 Top hits of RE02 in different plant species by BLAST searches.

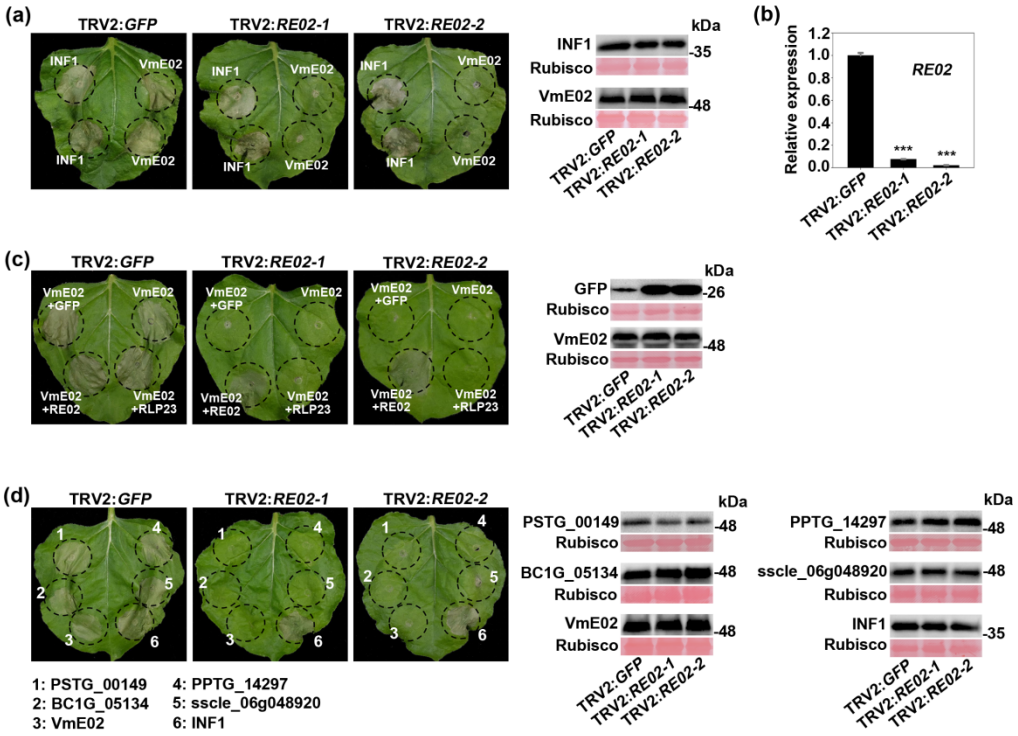

nph_16995_f1.tif

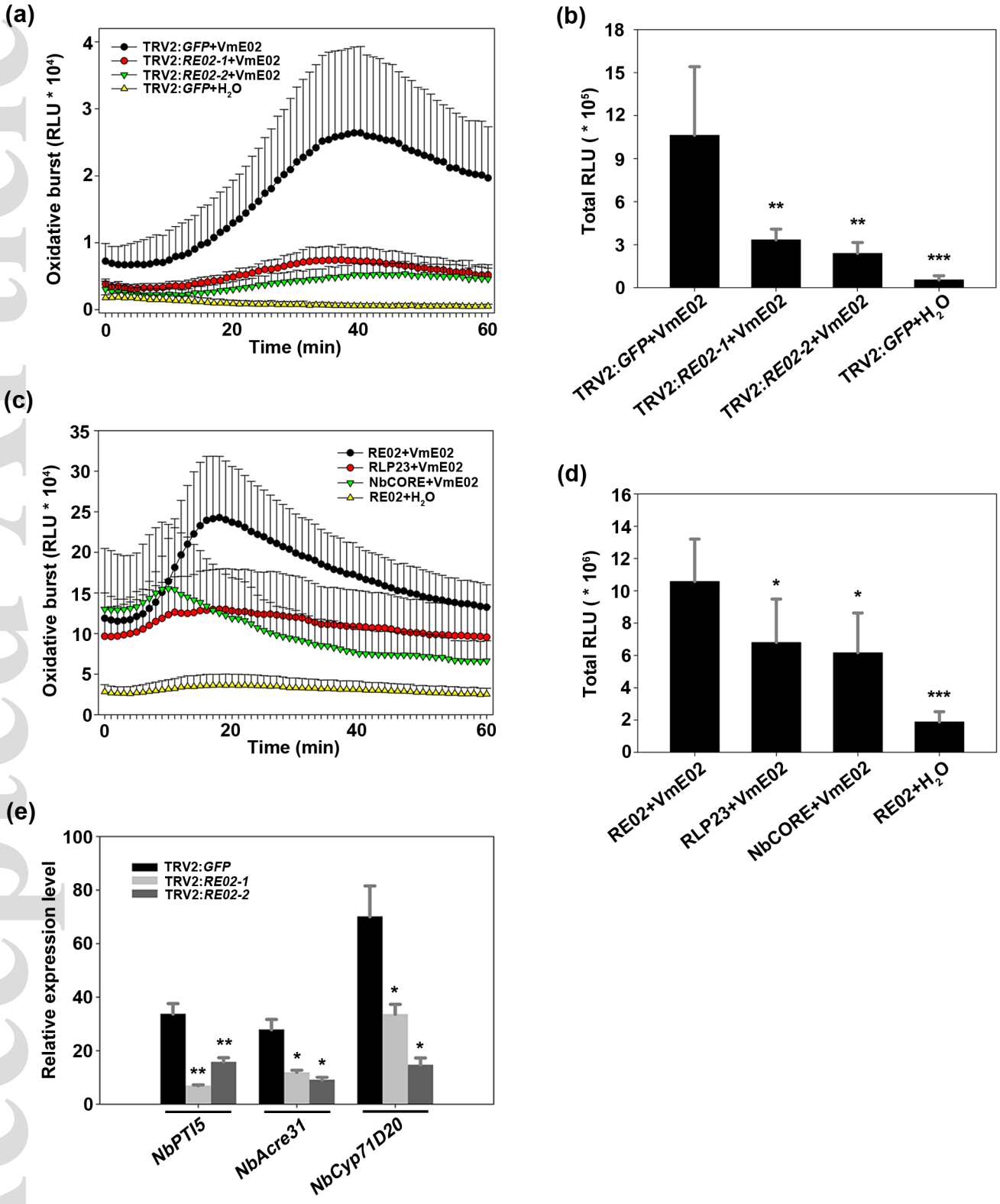

nph_16995_f2.tif

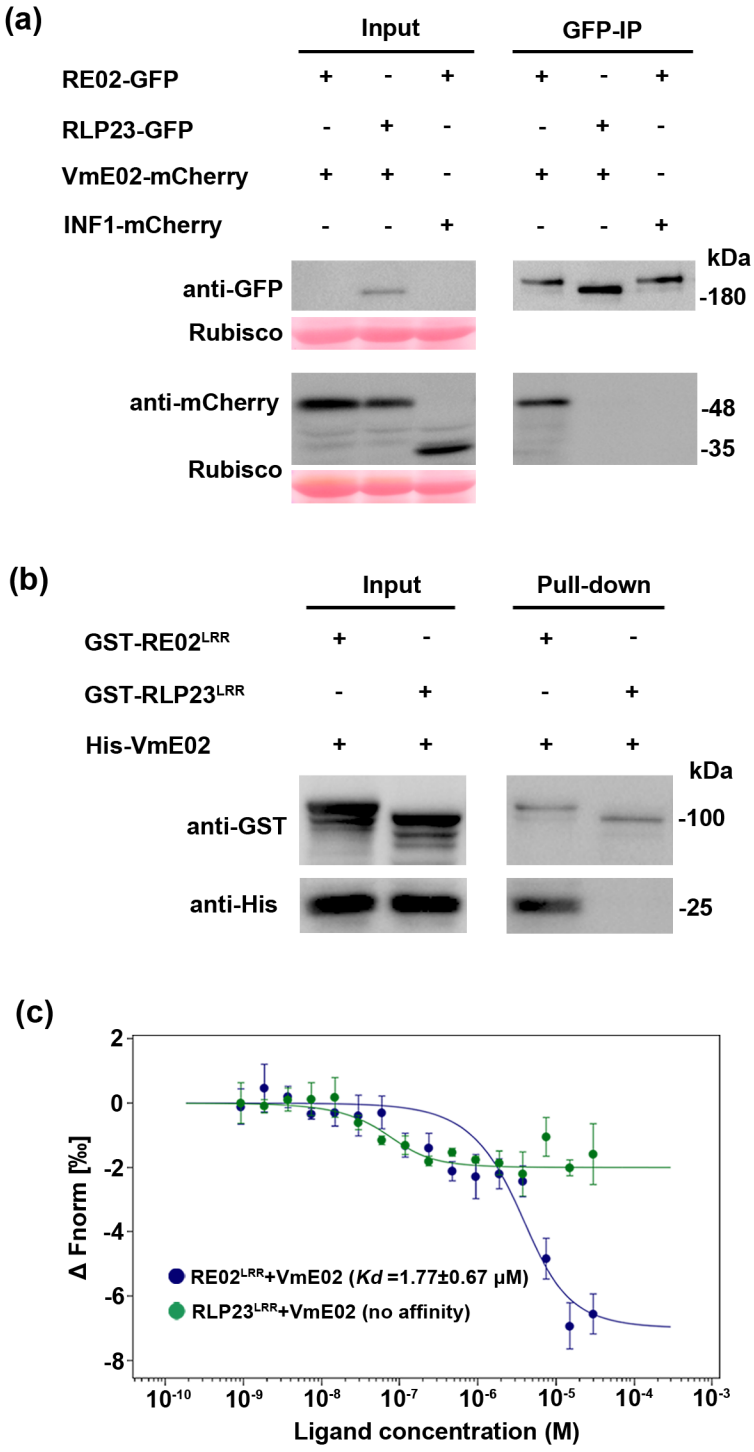

nph_16995_f3.tif

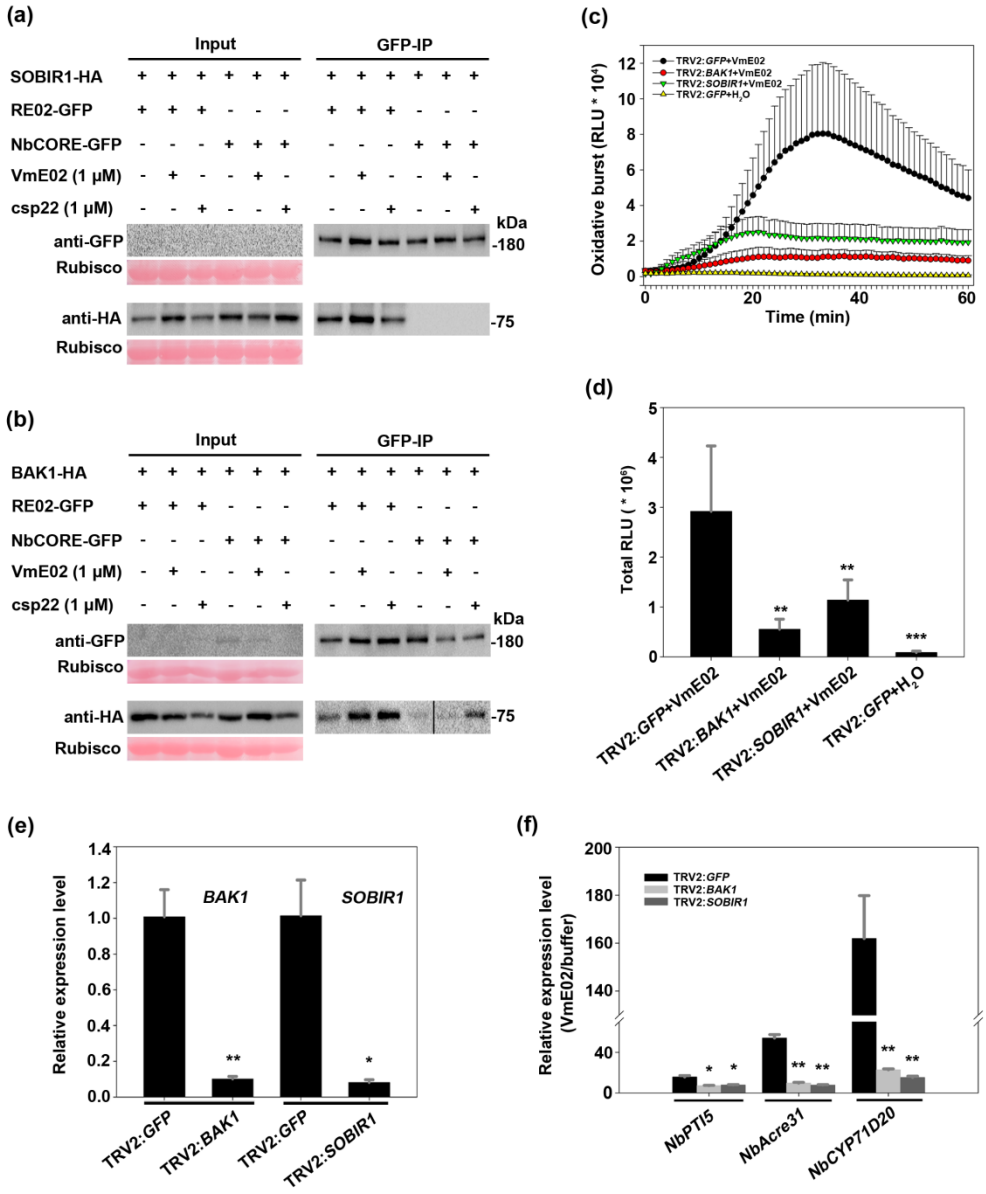

nph_16995_f4.tif

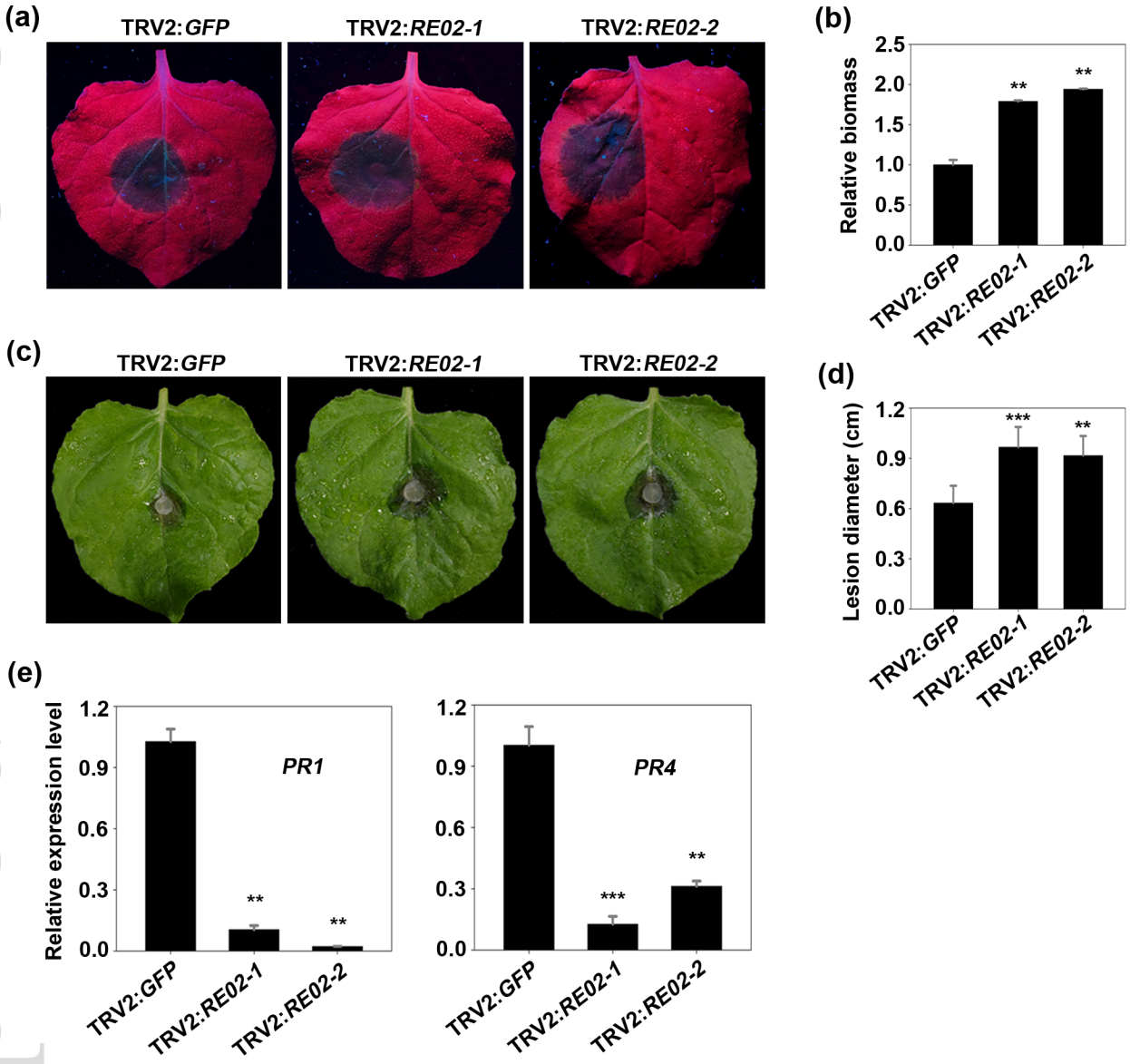

nph_16995_f5.tif

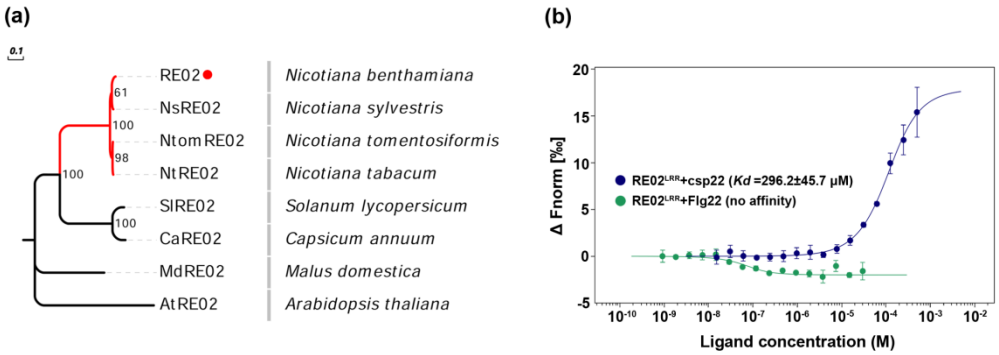

nph_16995_f6.tif